Adsorption of Hydrophilic–Hydrophobic Block Copolymers on Silica from Aqueous Solutions

Catherine Amiel

Groupe des Laboratoires de Thiais, 2 à 8 rue Henry Dunant, 94320 Thiais, France

Mohan Sikka,[†,‡] James W. Schneider, Jr., Yi-Hua Tsao,[§] and Matthew Tirrell*

Department of Chemical Engineering and Materials Science, University of Minnesota, Minneapolis, Minnesota 55455

Jimmy W. Mays

Department of Chemistry, University of Alabama at Birmingham, Birmingham, Alabama 35294

Received May 19, 1994; Revised Manuscript Received February 20, 1995[⊗]

ABSTRACT: Adsorption of a water-soluble diblock copolymer, poly(*tert*-butylstyrene)–sodium poly(styrenesulfonate) (PtBS–NaPSS), on silica surfaces in aqueous solutions was studied using ellipsometry and atomic-force microscopy (AFM). The block copolymers used were compositionally asymmetric, with large, hydrophilic, PSS blocks and small, hydrophobic, PtBS blocks. Materials with molecular weights of 87 000 and 160 000 were used. Adsorption could not be observed in pure water without added salt (NaCl). When the NaCl concentration was increased to 1 M, adsorption could be readily observed. The measured adsorbed amount at long times was significantly larger for the 87 000 diblock compared with that for a polyelectrolyte homopolymer of comparable molecular size, demonstrating the role played by the uncharged block in anchoring the diblock at the solid surface. The kinetics of adsorption showed a two-stage process: an initial diffusion-limited stage, followed by a slower buildup of surface coverage in a brush-limited stage. The number density of molecules at the surface was smaller for the higher molecular weight species, in agreement with simple scaling arguments.

Introduction

The amphiphilic nature of diblock copolymers is manifested in self-assembly phenomena in the presence of a selective solvent for one of the blocks, giving rise to formation of aggregates such as micelles, microemulsions, and, in the presence of a selective surface, adsorbed polymer layers.[1] This feature of diblock copolymers makes them attractive candidates for use as large surfactant molecules in applications such as colloidal suspension and the manipulation of surface properties.[2]

This study is concerned with the adsorption of diblock copolymers on nonpolymeric surfaces from a selective solvent for one block. The equilibrium properties and association kinetics of adsorbed layers of *neutral* diblock copolymers in nonpolar solvents have been discussed in several theoretical studies.[3–5] The adsorbed layer, at equilibrium, is considered to be divided into two regions: an anchoring film adjacent to the surface formed from the insoluble (B) block, and a solvated brush of the other (A) block (see Figure 1). The equilibrium adsorbed amount and layer thickness, from scaling arguments, are derived from a balance between the stretching energy of the solvated block, the interaction of the anchoring layer with the surface, and the consideration of thermodynamic equilibrium between the layer and the reservoir solution with chemical potential μ_{ex}. The process of layer formation at the solid interface is understood, broadly, as consisting of (a) an initial fast regime, during which single chains or micellar aggregates diffuse from the solution to fill up empty area on the surface, followed by (b) a slow buildup of surface density by the penetration of chains through the existing monolayer combined with molecular rearrangement to a brushy configuration for the solvated (B) layer. Various experimental studies are in qualitative agreement with these results.[6–10]

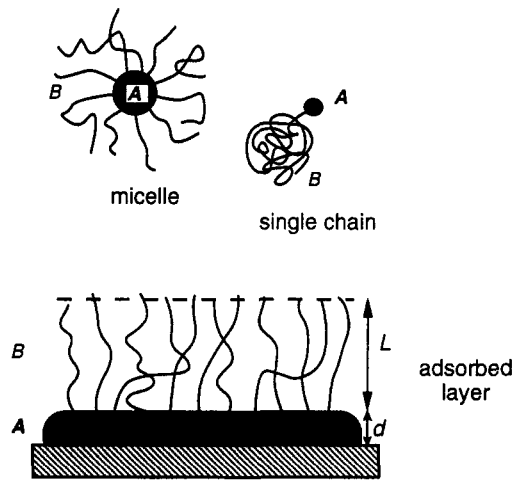

Figure 1. Diblock copolymers forming an adsorbed layer at a surface from a solution of micellar aggregates or single chains. The solvent is a precipitant for the A block while the B block is well solvated.

Colloidal particles are often suspended in aqueous solutions rather than in nonpolar solvents. For such systems, water-soluble chains, such as charged polymers, are required as stabilizers or flocculants. The chain configurations and, therefore, aggregation characteristics of polyelectrolytes differ from those of neutral

† This work forms part of the Ph.D. dissertation of Mohan Sikka.
‡ Present address: Department of Materials Science and Engineering, University of Pennsylvania, Philadelphia, PA 19104.
§ Present address: Polaroid Corp., Cambridge, MA 02154.
⊗ Abstract published in *Advance ACS Abstracts,* April 1, 1995.

0024-9297/95/2228-3125$09.00/0

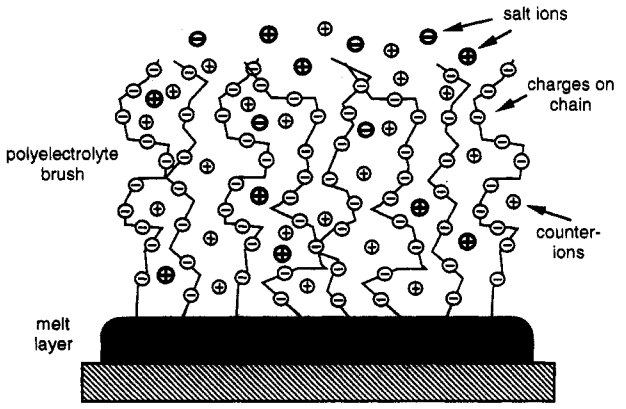

Figure 2. Neutral–charged diblock copolymers forming an adsorbed layer at a surface from an aqueous solution of the polymer. The anchoring layer is formed from the neutral, hydrophobic, blocks, while the polyelectrolyte blocks form a solvated brush in solution. Positive counterions that are found in conjunction with the negative charges on the polyelectrolyte disassociate in solution but remain within the volume of the layer for the solution conditions envisioned here. There are as many counterions as charges on the chain. The presence of salt is indicated by disassociated salt ions in solution.

polymers in good solvents due to the effect of electrostatic interactions. At high charge densities along the backbone and low ionic strength (corresponding to low salt concentration) in solution, electrostatic correlations between segments dominate chain configurations, leading to an increase in both the effective persistence length associated with the chain and the excluded volume in solution.[11–14] In the limit of no added salt, it is generally accepted that a highly charged polyelectrolyte at high dilution is stretched. As the salt concentration is increased, the range of electrostatic interactions begins to be reduced by screening effects, and the chain starts to recover its flexible nature. The interactions are completely screened at very high salt concentrations and the chain conformation resembles that of a neutral polymer. For example, poly(styrenesulfonate) has a Θ point (at which a neutral polymer chain exhibits a Gaussian configuration in solution) at an aqueous sodium chloride concentration of 4.2 M at 25 °C[15] and behaves like a neutral polymer in a good solvent at 0.15 M at 25 °C.[14]

The conformation of the polyelectrolyte chain can be reasonably expected to affect its adsorption behavior. This means that two additional factors, charge density along the chain and salt concentration, must be considered in the aggregation of charged polymers or neutral–charged diblock copolymers at interfaces. For example, for adsorption of homopolymer poly(styrenesulfonate) on silica from aqueous solution, there is no detectable adsorption in the absence of salt, a consequence of the strong repulsion between charged groups on the polyelectrolyte, and adsorbed amounts are found to increase with increasing ionic strength (salt concentration), a consequence of the screening effect of salt on electrostatic interactions.[16] The range of electrostatic interactions is also expected to affect the aggregation characteristics of neutral–charged diblock copolymers on surfaces from aqueous solutions. Theoretical attempts to examine the properties of such adsorbed layers have been undertaken recently, using scaling laws and self-consistent-field theory (SCF).[5,17] The layer is envisioned as consisting of an anchoring film of hydrophobic polymer at the solid surface and a brush of hydrophilic polyelectrolyte chains. The force of attraction to grafted

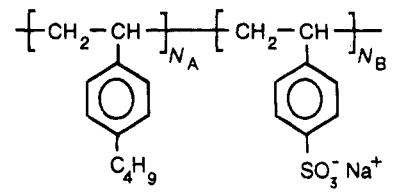

Figure 3. Molecular structure of neutral–charged block copolymer used in this study.

Table 1. Polymer Molecular Characteristics

sample	$10^{-3}M_w$	M_w/M_n	% of phenyl groups sulfonated on PSS block	N_{NaPSS}	N_{PtBS}
MT2	87	1.03	89	404	26
MT3	160	1.04	87	757	27
NaPSS	100	1.1	90	485	

polyions keeps the dissociated counterions within the volume of the brush.[18,19] These studies predict that the equilibrium adsorbed amount will decrease with decreasing salt concentration, and the brush thickness, for a given adsorbed amount, will increase as electrostatic interactions become more significant with decreasing salt concentration. Except for a recent study on adsorbed neutral–charged diblocks using the surface-forces apparatus,[20] evidence of experimental work in this area cannot be found in the literature. This work, using ellipsometry as the main analytical tool, constitutes a preliminary experimental study of the nature of the adsorption process for neutral–charged diblocks on surfaces from aqueous solutions.

Experimental Section

Materials. Diblock copolymers of poly(*tert*-butylstyrene)–sodium poly(styrenesulfonate) (PtBS–NaPSS) have been synthesized using methods described elsewhere.[20] To ensure the water solubility of the copolymers, these diblocks are highly asymmetric with a small hydrophobic PtBS block relative to the hydrophilic PSS block. In a water solution, the hydrophobic block will form a collapsed globule while the hydrophilic block will be solvated with a characteristic coil dimension that will depend on the size of the block and the salt concentration in solution.[14] Also, disassociation of the sodium counterions on the polyelectrolyte blocks will occur in solution. A NaPSS homopolymer of molecular weight 10^5 g/mol was also used. This was purchased from Polysciences Inc. The chemical structure of these diblock copolymers is shown in Figure 3 and the molecular characteristics of the polymers used in this study are summarized in Table 1.

Salt solutions were prepared from pure water obtained by distillation, deionization, and reverse osmosis. Salt solutions were prepared from sodium chloride obtained from Baker Inc. and filtered three times through 0.45 μm filters prior to use. Polymer solutions at a concentration of 1 mg/mL were prepared by dissolution in distilled water and equilibration for at least 1 week before any adsorption experiment. The polymer solutions were then diluted by the addition of water or 1 M salt solution to the required concentration and used for the experiment. To avoid dust particles, polymer solutions were filtered through 0.6 or 0.8 μm polycarbonate membrane filters from Nucleopore Inc. prior to each use.

Silica surfaces for adsorption were prepared in the following way. Polished silicon wafers (1.5–2 in.) were purchased from Virginia Semiconductor Co. The native oxide and any organic contamination on the surface of the wafers were removed by the following procedure: soaking in a 3:7 hydrogen peroxide/

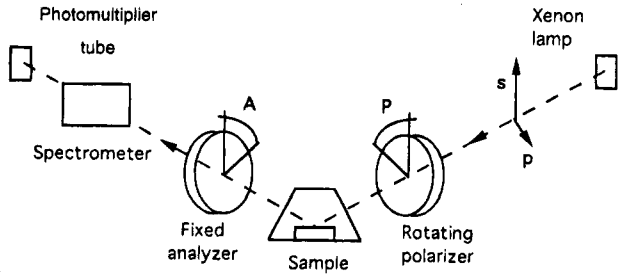

Figure 4. Schematic illustration of the experimental setup. The incident and reflected beams and the normal to the surface make up the plane of incidence.

sulfuric acid solution for 5 min, rinsing in deionized water for 5 min, etching in a 1:9 hydrofluoric acid/ammonium hydroxide solution for 30 s, rinsing again in water for 5 min, followed by careful drying using filtered nitrogen gas. A dense oxide layer of ca. 1500 Å thickness was then thermally grown on these wafers. The thickness and uniformity of this layer were checked using ellipsometry. All oxide surfaces were cleaned of any organic contamination using an ultraviolet lamp before each adsorption experiment.

Instrumentation. Adsorption experiments were performed using a SOPRA ES4G spectroscopic ellipsometer with a rotating polarizer and fixed analyzer (Figure 4). The light source is a xenon lamp (Hamamatsu Inc.) with an experimentally observable range of 250–800 nm. The polarizer is a quartz Rochon prism that is rotated at 40 cycles/s by a dc motor. The analyzer is a Glan–Taylor prism that is held fixed during the experiment but can be driven to its most sensitive position by a stepping motor. The spectrometer is a Czerny–Turner prism/grating system double monochromator for separating wavelengths with a resolution at 313 nm of less than 1 nm. Light is detected at the end of the optical train using a photomultiplier tube. A detailed description of spectroscopic ellipsometers and their operation can be found in the literature.[21]

The ellipsometric angles Δ and Ψ correspond to the change, on reflection, of the refractive phase and amplitude of p (parallel to the plane of incidence) and s (perpendicular to the plane of incidence) components of the light wave. Δ and Ψ are determined experimentally by the analyzer setting A with respect to the plane of incidence and the variation of the light intensity as the polarizer is rotated.[22]

Atomic-force microscopy (AFM) measurements on dried adsorbed layers were made by Dr. Yi-Hua Tsao at the Center for Interfacial Engineering (CIE), University of Minnesota, on a Nanoscope III microscope (Digital Corp., Santa Barbara, CA).

Experimental Procedure. All the ellipsometry measurements in this study were performed at 23 ± 2 °C at a wavelength of 589.3 nm and a fixed angle of incidence of 75.5°. Adsorption runs were performed as follows: Freshly cleaned substrates were placed in a specially built trapezoidal quartz cell with windows inclined to the base of the cell at a 75.5° angle. The cell was filled with pure water or a salt solution in water when measurements had to be made under these conditions or when the constancy of the ellipsometer readings with time had to be checked. Several quartz weights were placed on the substrates under all measurement conditions to ensure that the substrate did not drift in the cell with time. Water or salt solution could be drained from the cell without disturbing the wafer using a specially designed siphoning attachment. The cell was filled with polymer solution in pure water or with added salt when adsorption had to be studied as a function of time. Readings of Δ and Ψ could be taken as frequently as every 11 s if desired.

Data Analysis. The ellipsometry data were analyzed assuming a homogeneous layer for the polymer film. The refractive index n_1 and thickness d_1 of the polymer layer were determined from the basic equation of ellipsometry:[21]

$$\tan \Psi \, e^{i\Delta} = \frac{r_p}{r_s} = f(n_0, n_1, d_1, n_2, d_2, N_3, \lambda, \phi) \qquad (1)$$

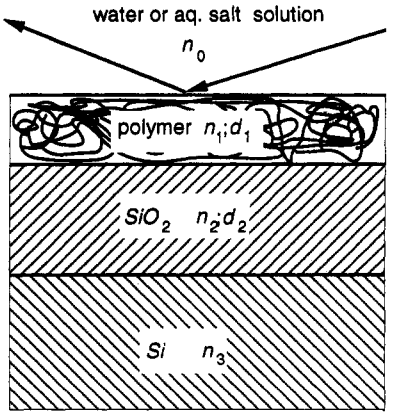

Figure 5. Multilayer model of adsorbed homogeneous polymer layer on silica used for data analysis.

Table 2. Refractive Index Increments in Water

species	dn/dc,[a] mL/g	ref
NaCl	0.165	26
MT2	0.152	this work
MT3	0.168	this work
PSS	0.180	this work

[a] Values at 25 °C.

r_p and r_s are the complex overall reflectances[23] for the multilayer system shown in Figure 5, parallel and perpendicular to the plane of incidence. They are a function of the (complex) refractive indices of all media, the layer thicknesses, the wavelength λ, and the angle of incidence ϕ. Equation 1 is a complex, nonlinear equation which is impossible to invert directly to determine the unknown film parameters, n_1 and d_1. The following iterative procedure was used:

The (complex) refractive index of the silicon underlayer, N_3, is known from literature values.[24] The refractive index used was $N_3 = 3.9702 - i0.03$ at $\lambda = 589.3$ nm. The thickness, d_2, and refractive index, n_2, of the dielectric SiO_2 layer were measured directly for each substrate in air. Although the thickness varied between samples, the refractive index of the silicon oxide was found to be $n_2 = 1.46 \pm 0.01$ at $\lambda = 589.3$ nm for all samples. This number agrees well with values published in the literature.[9] For estimating the refractive index of the solution in the cell, n_0, the contributions of all solution components (water, charged copolymer, and, in some experiments, salt) were considered.

$$n_0 = n_{\text{water}} + \left(\frac{dn}{dc}\right)_s c_s + \left(\frac{dn}{dc}\right)_p c_p \qquad (2)$$

where n_{water} is the refractive index of pure water (1.3327 at 23 °C),[25] $(dn/dc)_x$ is the refractive index increment of species x in water, and c_x is the concentration of species x. The subscripts s and p in this equation refer to salt and polymer, respectively. Table 2 lists the refractive index increments for each of the water-soluble species used in these experiments. The values for MT2 and MT3 were measured using an Abbe refractometer.

For pairs of values of the refractive index, n_1, and the adsorbed layer thickness, d_1, of the adsorbed polymer layer, Δ and Ψ could be calculated for the multilayer model depicted in Figure 5 using a well-established optical matrix formalism.[23] Software generated by McCrackin[27] was used to perform this calculation. A reasonable value of n_1 was assumed and a value of d_1 was found that minimized the difference between the calculated and experimental ellipsometric angles. Because the change in ellipsometric angles due to adsorption is small [$\sim O(1°)$] and taking into account the uncertainty in the ellipsometric angles [$\sim O(0.1°)$], unique values of n_1 and d_1 could not be found for any data set. Rather, a domain of corresponding values of n_1 and d_1 was generated. However, their product, which is related to the adsorbed amount of polymer, was found to be relatively invariant. For the calcula-

tion of the adsorbed amount, we have to consider the possibility that the adsorption of salt on the solid surface occurs. Frommer and Miller,[28] assuming a Donnan equilibrium between the adsorbed layer and the bulk phase, have derived relationships between the polymer adsorbed amount A and the salt adsorbed A_s. Positive polymer adsorption is generally accompanied by negative salt adsorption, i.e., depletion of salt, at the surface. We estimate that the extent of salt depletion is negligible for the salt concentrations used in our experiments. As in the case of adsorption without electrolyte, a simple equation can then be derived for the calculation of the polymer adsorbed amount A,[28,29] in mass per unit area:

$$A = \frac{d_1(n_1 - n_0)}{(dn/dc)_p} \tag{3}$$

where $(dn/dc)_p$ is the refractive index increment of the medium 0 due to the addition of polymer. Adsorbed amounts calculated in this way have an associated error of ±10%.

Results and Discussion

Adsorption Experiments Using Ellipsometry. Adsorption measurements were first made in water without added salt. The following procedure was used: ellipsometry measurements were taken on a silica substrate immersed in pure water. The adsorption cell was then drained, the cell was refilled with a block copolymer solution of concentration 60 ppm (weight/weight) in water, and measurements were taken as a function of time.

A similar experiment was conducted in a 1 M aqueous NaCl solution. In this case, initial measurements were taken on a silica substrate immersed in salt solution with no added polymer. The adsorption cell was then drained, the cell was refilled with a 1 M aqueous NaCl solution containing block copolymer at a concentration of 60 ppm, and measurements were taken as a function of time.

Representative data sets are shown in this section. Figure 6 shows the variation with time of the ellipsometric parameters tan Ψ and cos Δ for the MT3/water and MT3/aqueous salt solution systems. Values were recorded every 11 s for the first 1.5 h and then less frequently, as appropriate. Data for the first 1.5 h are shown in this plot. The zero on the x axes marks the point in time when polymer solution was added to the cell (t_0). Values of tan Ψ and cos Δ shown at t_0 are for initial measurements in water or aqueous salt solution without polymer. We can clearly deduce from this figure that, in the absence of salt, there is insufficient aggregation of polymer at the silica surface to cause an observable change in the ellipsometric parameters. However, at a salt concentration of 1 M, a decrease in cos Δ and a complementary increase in tan Ψ occur after addition of the polymer solution, indicating a growing layer.

A noteworthy point is that the two sets of data (i.e., with and without salt) encompass different ranges in the values of the ellipsometric parameters because the addition of salt significantly alters the refractive index of water (see Experimental Section). By inference, the absence of an observable change in tan Ψ and cos Δ in salt-free solutions before and after addition of polymer indicates that the refractive index of the solution medium is not significantly altered by the dissolution of polymer at the concentrations used in this study. All changes on replacing polymer-free solutions with solutions containing polymer must, therefore, be a consequence of adsorption at the silica surface.

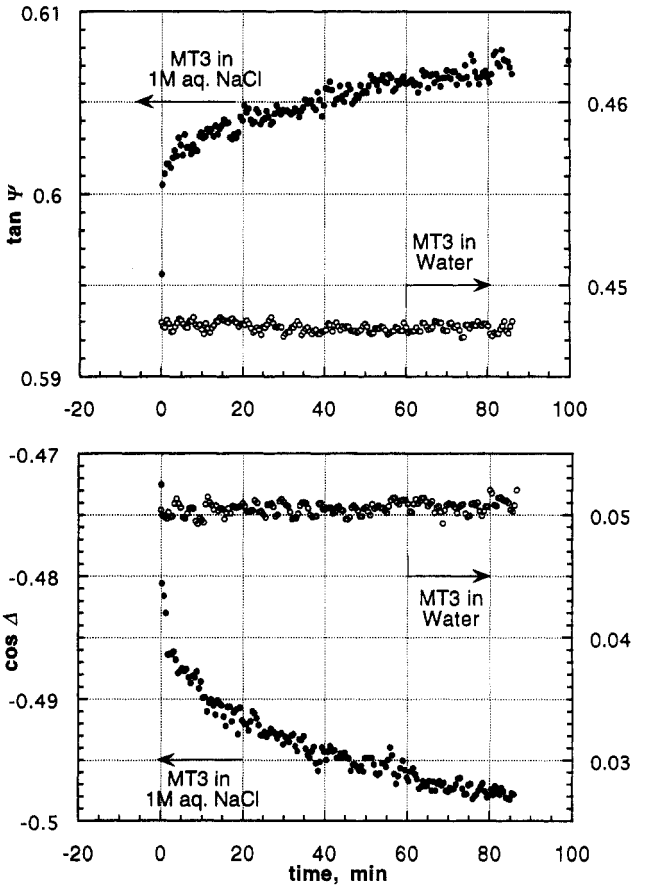

Figure 6. Variation of ellipsometric parameters as a function of time for adsorption of MT3 (neutral−charged diblock) on a silica surface from aqueous solutions of polymer. The polymer concentration in solution was 60 ppm (weight of polymer/weight of solution).

For both block copolymers, adsorption data were collected for up to 10 h at a polymer concentration of 60 ppm in 1 M salt solutions. Ellipsometry measurements were also taken for adsorption of PSS (dry $M_w = 10^5$) at a polymer concentration of 60 ppm in 1 M salt, in order to contrast block copolymer adsorption behavior with that of homopolymer polyelectrolyte. Figure 7 compares the variation of tan Ψ and cos Δ for MT2 and PSS as a function of time under similar solution conditions. Clearly, the homopolymer polyelectrolyte, whose molecular size is comparable to that of the charged block in MT2, shows a smaller extent of adsorption than MT2.

For the MT3 system, measurements in 1 M salt were also taken at polymer concentrations of 60 and 300 ppm in order to elucidate the effect of increasing concentration on the kinetics and extent of adsorption. All of these concentrations are above our best estimates of the critical micelle concentrations for these molecules (≈2 ppm for MT2) discussed further in the next section.

In all experiments with salt, the following experimental protocol was observed: readings in 1 M salt solution were taken until the ellipsometric parameters had reached a plateau value for adsorption (typically, for about 10 h; part I of experiment). The cell contents were then drained and replaced with pure water, and measurements were taken for up to 15 h in water (part II of experiment). The cell was then drained once again and refilled with 1 M salt solution, and measurements were continued (part III of experiment). Differences in tan Ψ and cos Δ values between parts I and II are mainly due to the difference in refractive index between

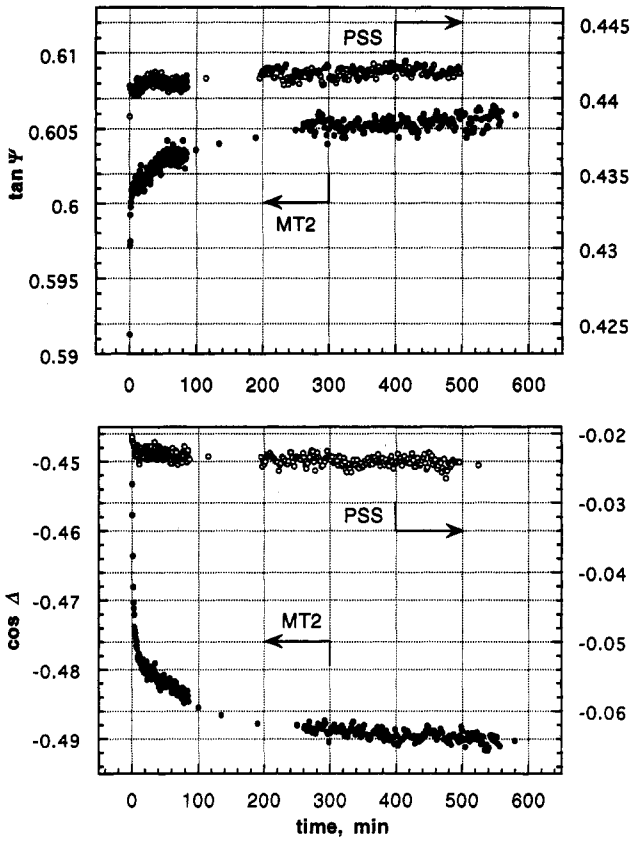

Figure 7. Variation of ellipsometric parameters as a function of time for adsorption of MT2 diblock and PSS homopolymer of comparable size from aqueous solutions of polymer. The polymer concentration in solution was 60 ppm in both cases, and NaCl was present at a concentration of 1 M.

1 M salt solutions and pure water. A comparison of terminal tan Ψ and cos Δ values measured in 1 M salt before and after the addition of water, i.e., in parts I and III of the experiment, provides an indication of whether any desorption of polymer took place in water. Figure 8 shows typical data for such an experiment. In this example, part I corresponds to the adsorption of MT3 at a polymer concentration of 60 ppm in 1 M salt. Terminal cos Δ values in parts I and III are indistinguishable within experimental error. tan Ψ values in III are somewhat lower than in I. This difference is largely because polymer is added to the 1 M salt solution in I as a solution in water, with the volume of additional water + polymer being ~5% of the total volume of solution. This causes the molarity, and, hence, refractive index, of the solutions between I and III to differ by a corresponding amount. The tan Ψ values, which are extremely sensitive to the refractive index of the solution, reflect this difference. A qualitative conclusion from the data, then, is that large amounts of desorption do not take place in water in the time scale of the experiment, although a calculation of the adsorbed amount before and after "rinsing" with water is required to confirm this quantitatively.

Calculation of Adsorbed Amounts. Table 3 shows the adsorbed amount calculated from the experiments described in the previous section for each of the polymer systems studied. Only *final* adsorbed amounts calculated from data taken at long times under different adsorption conditions are listed here. The methodology outlined in the Experimental Section was used in calculating the adsorbed amounts from the ellipsometry data.

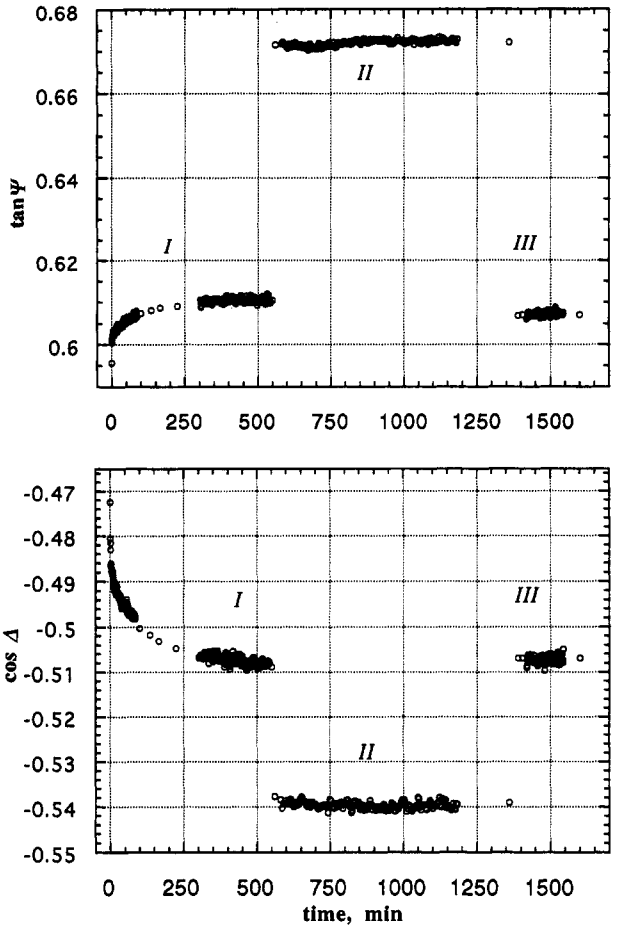

Figure 8. Variation of ellipsometric parameters as a function of time for adsorption of MT3 from aqueous solutions of polymer. The polymer concentration in solution was 60 ppm in both cases, and NaCl was present at a concentration of 1 M. Data collected for the entire experiment are shown. The three parts of the experiment are (I) adsorption in 1 M salt solution, (II) cell contents drained and replaced with salt-free water, and (III) water drained and replaced with 1 M salt solution.

Table 3. Adsorbed Amounts for Polymers

polymer	adsorption medium	conc, ppm	adsorbed amounts,[a] A, mg/m^2 before rinsing with water	adsorbed amounts,[a] A, mg/m^2 after rinsing with water
NaPSS	water	60	*b*	
	1 M aq salt soln	60	0.45	0.45
MT2	water	60	*b*	*b*
	1 M aq salt soln	60	2.1	1.9
MT3	water	60	*b*	*b*
	1 M aq salt soln	60	1.8	1.9
	1 M aq salt soln	300	1.8	1.8

[a] Calculated adsorbed amounts have an average associated error of 10%. [b] No adsorption could be measured.

The following observations can be made from these results:

(a) No adsorbed amount could be measured for polyelectrolyte homopolymer or neutral–polyelectrolyte block copolymer in pure water without added salt. It seems logical to conclude that repulsion between charged groups on the polyion chain or block in the absence of electrostatic screening inhibits polymer accumulation at the solid–solution interface.

(b) At a salt concentration of 1 M, electrostatic interactions are screened sufficiently to allow aggregation of polymer at the solid surface; adsorbed amounts

can now be measured from ellipsometric data. Semiquantitatively, this can be understood as follows: the range of repulsive interactions in the presence of dissolved salt is given by the Debye length κ^{-1}, where $\kappa^2 = 8\pi I l_B$; I is the ionic strength of the solution, and the Bjerrum length, l_B, is given by $l_B = e^2/\epsilon T$, where e is the electronic charge, ϵ is the dielectric constant of the solvent, and T is the temperature in energy units. For distances larger than κ^{-1}, electrostatic interactions in solution are considered to be screened. The Debye length should be compared to the effective distance between repulsive charges on the polyelectrolyte chain. This would be the monomer length (~3 Å) for the charge densities considered, except that counterion condensation[30] reduces the effective polymer charge for distances smaller than l_B (~8 Å). The Bjerrum length is, therefore, the appropriate length scale for electrostatic repulsion along the chain. At 25 °C, κ^{-1} changes from around 30 Å at a sodium chloride concentration of 0.01 M to 10 Å at 0.1 M, and 3 Å at 1 M. At 1 M, then, the Debye screening length is smaller than l_B, and the conformational and aggregation properties of the polyelectrolyte chain or block should resemble those of a neutral chain in moderate-to-good solvent conditions.

(c) Adsorbed amounts are 4–5 times higher for MT2 than for PSS homopolymer of molecular size comparable to that of the charged block in MT2 for adsorption from a 60 ppm solution in 1 M salt. This indicates that the short, hydrophobic, PtBS block in MT2 plays a role in anchoring the block copolymer to the wafer surface: such a configuration is logical since it would minimize the (unfavorable) contact between the hydrophobic block and the aqueous solution. However, a more detailed description of the structure of the adsorbed layer is difficult to deduce from the adsorbed amount alone. In particular, the inability to estimate a unique value of the thickness of the adsorbed layer makes it impossible to infer a detailed conformation of the polyelectrolyte block of an adsorbed molecule from the ellipsometry data, including whether it plays a role in anchoring the molecule to the surface.

(d) For MT3, no increase in the maximal adsorbed amount in 1 M salt is found when the polymer concentration in solution is increased by fivefold (from 60 to 300 ppm). This suggests that the adsorbed amount is independent of polymer concentration in solution for the range of concentrations studied here, although more data need to be taken at varying concentrations to confirm this.

(e) Within experimental error, calculated adsorbed amounts for the block copolymers are unchanged for measurements taken before and after filling the cell with pure water for up to 10 h. This shows that the rate of desorption in water, if any, is slow and also that the energy of adsorption of the hydrophobic block is large enough to compensate for the electrostatic repulsion among charged segments in pure water, the expectation being that the repulsion would favor desorption.

The difference in surface coverage between MT2 and PSS homopolymer was confirmed qualitatively with atomic-force microscopy (AFM) measurements on dried layers. Wafers were immersed for 24 h in 1 M solutions containing polymer at 60 ppm. These were then rinsed thoroughly with deionized water and allowed to dry in a vacuum oven for 1 day before AFM measurements were carried out. Figures 9 and 10 show AFM scans on the surface of the dried wafers for PSS and MT2,

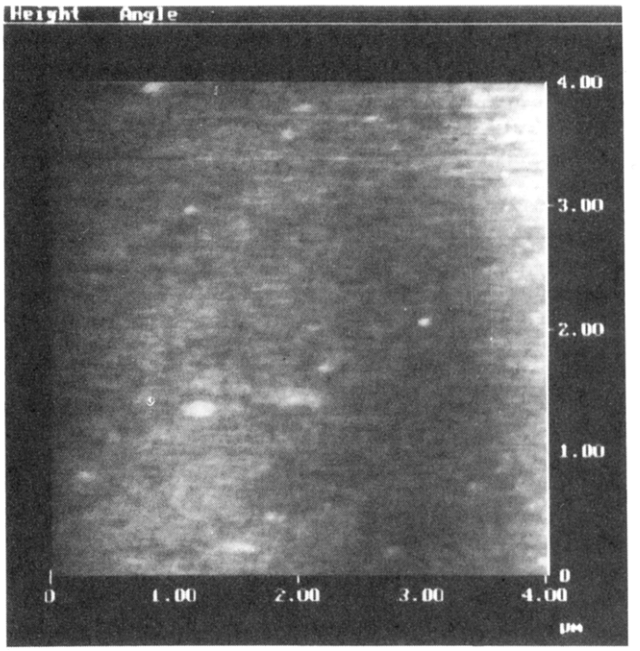

Figure 9. Atomic-force microscopy scan of the surface of a wafer immersed in an aqueous solution of PSS homopolymer for 24 h. The surface was rinsed and dried before the AFM measurement. The polymer concentration in solution was 60 ppm, while the salt concentration was 1 M. The molecular weight of the polymer is comparable to that of the PSS block in MT2 (see Table 1). The size of the sampled surface is 4 μm × 4 μm, and the vertical scale is from 0 to 50 Å. The root-mean-square roughness for this image is around 2 Å, which is comparable to that for a bare silica surface.

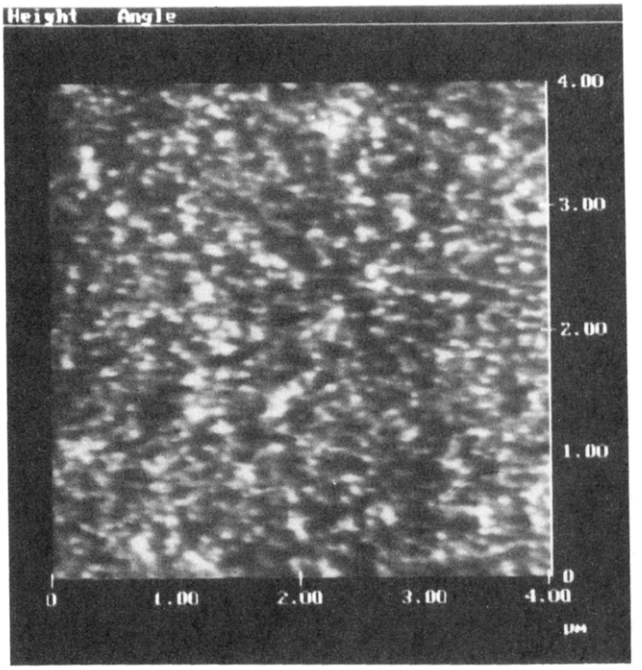

Figure 10. Atomic-force microscopy scan of the surface of a wafer immersed in an aqueous solution of MT2 for 24 h. The surface was rinsed and dried before the AFM measurement. The polymer concentration in solution was 60 ppm, while the salt concentration was 1 M. Significant aggregation of polymer on the surface was detected. The size of the sampled surface is 4 μm × 4 μm, and the vertical scale is 100 Å. The root-mean-square roughness for this image is around 5 Å.

respectively. Clearly, the MT2 surface shows significant texture suggestive of aggregation of polymer whereas the PSS surface shows no texture and appears to be very similar to a bare silica surface.

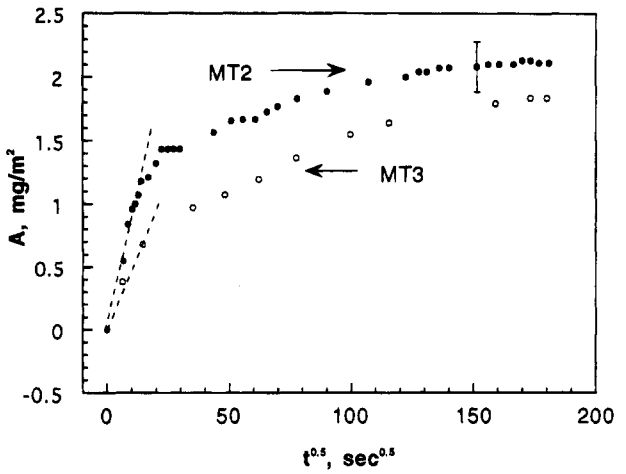

Figure 11. Mass adsorbed amounts, A, for the neutral–charged diblocks versus the square root of time in seconds, calculated from ellipsometric parameters for long measurement times. The polymer concentration in aqueous solution was 60 ppm, while the salt concentration was 1 M. In the early stage a transport-limited increase in the surface coverage is seen. At later times, a slowing down of the layer growth occurs until a saturation value of A is reached.

Adsorption Kinetics: Transport-Limited Regime. A qualitative feature of all adsorption measurements for neutral–charged diblocks in 1 M salt is that the amount of adsorbed polymer increases monotonically with time and reaches a plateau value. This is apparent without detailed analysis of the ellipsometric data. In the early stages of the experiment, a rapid change in the ellipsometric parameters suggests that the formation of the adsorbed layer may be controlled by diffusion of material to the solid surface. In order to check that the experimental observations are consistent with the notion of transport-limited growth, an expression for the increase of the adsorbed amount with time, $A(t)$, is required; this may be arrived at by integrating the flux of material to the surface, $j_{surface}$, with respect to time:[9,31]

$$A(t) = \int_0^t j_{surface}\, dt = \frac{2}{\pi^{1/2}} c_0 (Dt)^{1/2} \qquad (4)$$

where D and c_0 are the diffusion component and the concentration of the adsorbing species in solution, and $j_{surface}$ is determined as a function of system parameters by solving Fick's second law with appropriate boundary conditions:

$$\frac{\partial c(x,t)}{\partial t} = D\frac{\partial^2 c(x,t)}{\partial x^2} \qquad (5)$$

$$c(x=0,t) = 0 \qquad c(x,t=0) = c_0 \qquad (6)$$

Figure 11 shows calculated adsorbed amounts for MT2 and MT3 plotted versus $t^{1/2}$ for experiments at a polymer concentration of 60 ppm in 1 M salt. An initial linear regime, where the adsorption rate is controlled by diffusion of polymer to the interface, is indicated by this data, though it does not endure long. By inference, other processes, such as desorption and molecular rearrangement, are not rate-limiting in the diffusion regime, and the probability that polymer reaching the surface is adsorbed rapidly is high. It is important to note that the dynamics of the growth of the adsorbed layer in the diffusion-controlled regime for the block copolymer appear very different than those for the initial stages of PSS homopolymer adsorption (see Figure 7); for the same adsorption time, adsorbed amounts are larger for the block copolymer than for a homopolymer of comparable size. This indicates that the physical attachment of the small hydrophobic block to the surface significantly increases the adsorption potential in the case of the diblock.

The slope of A versus $t^{1/2}$ in the early regime provides a measure of the diffusion coefficient for the transport of material to the solid surface, provided the appropriate concentration is used for the value of c_0 in eq 4.

The critical micelle concentration (cmc), the lowest polymer concentration at which micellar aggregates will begin to form at equilibrium, is very small for MT2 and MT3. For MT2, the cmc in water solutions has been estimated at a polymer concentration of 2 ppm (weight/weight) from fluorescence experiments.[32] This indicates that solutions used for adsorption experiments, at concentrations of 60 ppm or higher, will contain micelles in equilibrium with free chains. In this light, a critical question is whether adsorption in the diffusion-limited regime takes place by transport of single chains or of micelles to the wafer surface. This question can, in theory, be answered by the calculation of the diffusion coefficient, D, from the linear portion of the A versus $t^{1/2}$ plot. This value could then be compared to estimates for the diffusion coefficient for micelles and single chains in order to discriminate the adsorbing species, the diffusion coefficient being somewhat lower for the more massive micelles. Unfortunately, data resolution in the first few points in Figure 11 is too poor to allow determination of D with the required accuracy. Also, the choice of the concentration of single chains (cmc) or the concentration of micelles (the difference between the solution concentration and the cmc) for c_0 in eq 4 gives a corresponding low or high value for D, making a critical comparison difficult. However, the qualitative trend from Figure 11 is clear: larger aggregates or free chains associated with MT3 (larger molecular size) adsorb the wafer surface at a slower rate than those associated with MT2 (smaller molecular size).

Adsorption Kinetics: Brush-Limited Regime. Increase in surface coverage beyond the transport-limited regime is understood as follows: The growth of the adsorbed layer by diffusion of material to the wafer surface will continue until empty area on the surface has been filled up. After this, adsorption of additional polymer at the surface will require penetration of chains through the potential barrier created by chains already at the surface, and a significant slowing down of the rate of adsorption has to take place. The deviation of the A versus $t^{1/2}$ plot from linearity (see Figure 11) marks the end of the transport-controlled regime, and the adsorbed amount at this point, A_{diff}, can be used to calculate the average spacing, Σ_{diff}, between chains at this transition. The average intermolecular spacing, Σ, for a given adsorbed amount, A, is given by

$$\pi\left(\frac{\Sigma}{2}\right)^2 = \frac{M}{AN_{Av}} \qquad (7)$$

where M is the molecular weight of the block copolymer and N_{Av} is Avogadro's number.

Table 4 shows that Σ_{diff} has a value between R_g and $2R_g$, where R_g is the radius of gyration of the PSS block in a 1 M NaCl solution. This demonstrates that eq 4 describes the increase in surface coverage for relatively little interaction between adsorbed macromolecules. At

Table 4. Molecular Parameters for MT2 and MT3 in 1 M Salt

polymer	R_g,[a] Å	Σ_{diff},[b] Å	Σ_{sat},[c] Å	$R_{H,micelle}$,[d] Å
MT2	100	125	90	160
MT3	150	210	130	450

[a] Radius of gyration of polyelectrolyte block calculated at a salt concentration of 1 M in dilute solution using the wormlike model for the polymer conformation.[14] [b] Average spacing between adsorbed chains calculated at the end of the transport-limited regime for adsorption at 60 ppm polymer concentration (Figure 11). [c] The same quantity calculated at the maximal adsorbed amount for adsorption at 60 ppm polymer concentration (Figure 11). [d] Hydrodynamic radius of block copolymer micelle measured in solution.[32]

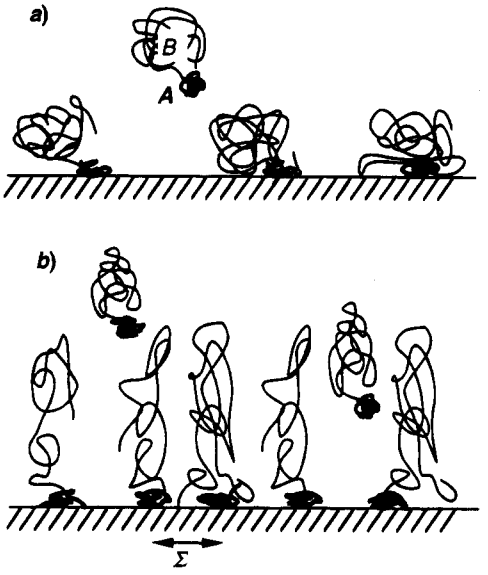

Figure 12. Schematic model for the two regimes of adsorption for neutral–charged (A–B) diblocks in aqueous solutions at high salt concentrations. (a) The diffusion-limited regime with a rapid growth of adsorbed macromolecules. Chains are relatively unperturbed from their solution configuration. (b) The brush-limited regime with slowing down of adsorption with increased surface coverage. Overlapping coils are stretched away from the surface. Σ is the average distance between adsorbed molecules along the surface.

this low coverage, the polyelectrolyte chains are, on average, widely enough separated so that their conformation on the surface is not perturbed significantly from their conformation as free chains in solution.[33] This situation changes when the average distance between adsorbed chains becomes smaller than the size (diameter) of the polyelectrolyte coil in solution. Chains begin to overlap on the surface and the increased osmotic pressure in the solvated layer causes the polyelectrolyte coils to swell into the reservoir of solvent. The swelling involves the stretching of chain conformations and the creation of a brushy conformation (Figure 12).[33] The energetics of increasing surface coverage in this brush-limited regime must balance the energy cost associated with chain stretching with the gain in energy due to adsorption at the wafer surface. Chains from the solution have to penetrate the potential barrier created by the brush in order to reach the surface, and this becomes progressively more difficult as increased coverage increases the stretching penalty. As a consequence, the adsorption is expected to slow down and approach a saturation value in this regime. Figure 11 shows that the experimental data follow this trend for adsorption at long times. Σ_{sat}, the average distance between adsorbed chains at saturation for adsorption at 60 ppm,

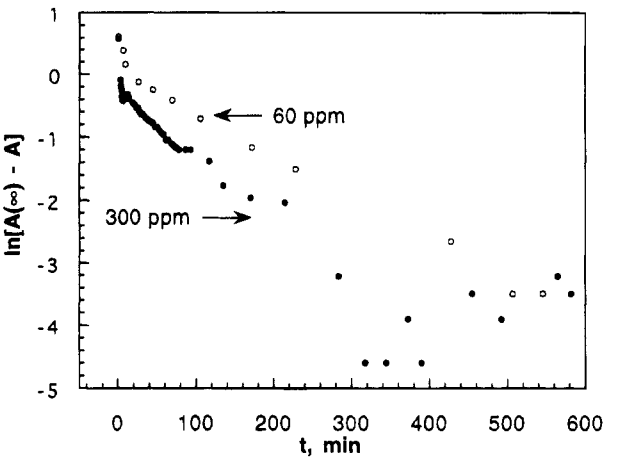

Figure 13. Long-time behavior of the adsorption for MT3 for two different polymer concentrations in 1 M aqueous salt solutions. $A(\infty)$ is the adsorbed amount at saturation (infinite times). In the earliest stages, the diffusion-limited regime is seen. At longer times, the increase of the adsorbed amounts is described by an exponential law, and the slope of the plot gives the rate constant, k, of the adsorption process.

is listed for each polymer system in Table 4. The increase of the adsorbed amount in the brush-limited regime is expected to follow an exponential time dependence that describes the slowing down of the adsorption process in this regime. This may be written as[4,31]

$$A(t) = A(\infty)(1 - e^{-kt}) + \tilde{A} \qquad (8)$$

where $\tilde{A}$ indicates the adsorbed amount that must be reached for the exponential law to be valid and k is the rate constant of the adsorption process in the brush-limited regime.

Figure 13 shows the long-time behavior of the adsorption of MT3 for two different polymer concentrations in 1 M aqueous salt solutions. In the early stage, the $t^{1/2}$ behavior can be seen, followed by the exponential behavior described by eq 8 for longer times. The slope of the lines for the brush-limited regime gives the rate constant, k, for the adsorption process in this regime. The rate constants for the two concentrations are different, even though the adsorbed amounts at saturation are indistinguishable within experimental error (see Table 3). From the plots in Figure 13, $k = 1.1 \times 10^{-4}$ s^{-1} for a polymer concentration of 60 ppm and 1.7×10^{-4} s^{-1} for 300 ppm. The increase in the rate constant with concentration can be explained as follows: as the concentration in the solution is increased, there are statistically more molecules hitting the surface at any given time, leading to a faster rate of growth of the adsorbed layer and a higher value of k at higher concentration. It is also possible that the slower long-time behavior is related to some sluggish rearrangement or dynamics in the adsorbed layer such as reorganization of adsorbed micelles. Both this and the barrier developed by constructing the brush may dictate the long-time behavior.

Independent evidence for stretching of the PSS block can be found in a recent study using the surface-forces apparatus on adsorbed layers of MT2 on mica in 1 M aqueous salt solutions.[20] The surface coverage was reported to be around 1.5 mg/m^2. The onset of repulsive forces between two such adsorbed layers was reported at a distance of 400 Å between the mica surfaces. This corresponds to a layer height of 200 Å, about twice the radius of gyration of the PSS block in a 1 M solution.

At the values of surface coverage reported in this study, the layer height for the same system is expected to be 10% larger based on theoretical predictions, although unique determination of layer thicknesses has not been possible using ellipsometry.

Finally, it is important to note from Table 4 that the size of the solvated coil (R_g), rather than the size of the micelle ($R_{H,micelle}$), provides the better estimate of the intermolecular distance at which overlap between adsorbed chains begins (Σ_{diff}). This suggests either that transport of free diblock chains to the wafer surface is the dominant process for layer growth in the diffusion-limited regime or that diffusion of micellar aggregates to the surface is followed by reorganization of the micelles into single adsorbed chains at the surface.

Variation of Adsorbed Amount with System Parameters. The dependence of the equilibrium adsorbed amount on the size of the photoelectrolyte block and the salt concentration can be predicted by constructing an expression for the grand canonical free energy, G, for the polymer brush in contact with a reservoir of solution. This procedure follows the analysis of Marques et al. for adsorption of neutral diblock copolymers from a selective, nonpolar, solvent for one block,[3] extended to neutral–charged diblocks in aqueous solutions by Dan and Tirrell.[17] The physical model for the adsorbed layer is that depicted in Figure 12b, rather than the one in Figure 2, since the small hydrophobic blocks are not expected to form a complete wetting layer at the adsorbed amounts measured. The polyelectrolyte chains in this analysis are envisioned as being grafted on the solid surface via the adsorbed hydrophobic block. The total free energy per unit area is given by

$$G = \sigma\left(-\delta + \frac{N_B\sigma^{5/6}}{\phi_s^{2/3}} - \mu_{ex}\right) \tag{9}$$

where $\sigma \sim$ the number density of chains on the surface, i.e., the number of chains per unit surface area, $-\delta$ is the energy gain per chain due to attachment of the hydrophobic block on the surface, and μ_{ex} is the chemical potential of the solution. $N_B\sigma^{5/6}/\phi_s^{2/3}$ is the free energy per grafted polyelectrolyte block,[33,34] N_B segments in size, in a swollen brush (Figure 12b). The brush is in contact with an aqueous solution at a salt concentration given by ϕ_s. The inclusion of the salt concentration in the free energy expression indicates that, in the case of polyelectrolytes in contact with ionic solvents, electrostatic interactions between charged segments contribute to the stretching energy of the grafted chain. An assumption in this analysis is that the energy of interaction of the hydrophobic block with the surface can be approximated by a constant and does not depend on the size of the block; for the materials used in this study, this assumption is justified by the small, and equal, size of the PtBS block for both MT2 and MT3.

For the range of polymer concentrations studied here, the adsorbed amount at saturation seems to be insensitive to the solution concentration c_0. This suggests that the chemical potential in the solution, μ_{ex}, which should change with c_0, is small and can be neglected in the overall energy balance. Thus, the equilibrium surface coverage is covered by the balance between the energy of adsorption of a diblock and the free energy of the polyelectrolyte brush. Minimizing G with respect to σ gives

$$\sigma \sim \phi_s^{4/5}\left(\frac{\delta}{N_B}\right)^{6/5} \tag{10}$$

The height of the equilibrium brush, L_B, is then given by

$$L_B = N_B\left(\frac{\sigma^{1/3}}{\phi_s^{2/3}}\right) \tag{11}$$

or

$$L_B = N_B^{3/5}\left(\frac{\delta}{\phi_s}\right)^{2/5} \tag{12}$$

The adsorbed amount, A, in weight of polymer adsorbed per unit area, is given by

$$A \sim \sigma N_B \tag{13}$$

or,

$$A \sim \phi_s^{4/5}\left(\frac{\delta^{6/5}}{N_B^{1/5}}\right) \tag{14}$$

Equation 10 predicts that the number of molecules absorbing per unit area decreases as $N_B^{6/5}$ with increasing polyelectrolyte block length, a consequence of the fact that longer chains pay a higher energetic penalty for stretching than do shorter chains for the same number density of molecules at the surface, σ, and the same salt concentration. The mass density, A, shows a weaker dependence, however, decreasing only as $N_B^{1/5}$ with increasing polyelectrolyte block length.

Experimental results from this study are in qualitative agreement with these predictions: According to eq 13, mass of polymer adsorbed per unit area (A) should be ca. 13% higher for MT2 than for MT3 on account of the difference in PSS block length between these systems, all solution conditions being similar. Experimentally, a range of 5–15% is calculated from different experiments. It needs to be noted that values of A are measured with an average error of 10%, which is comparable to the expected difference in A between the two systems from scaling arguments. However, experimental values appear to be systematically lower for MT3, as can be seen in Figure 11. More importantly, eq 10 predicts that the ratio of the *number of chains* per unit area (σ) should be around 2:1 for MT2 versus MT3. This is the result that is seen experimentally, with statistical significance well outside the bounds of experimental error.

The effect of salt concentration is expected to become significant when local flexibility in the polyelectrolyte brush starts to be affected by electrostatic interactions. Quantitatively, one may compare the intrinsic segment length of PSS, L_P, which is around 12 Å,[14] with the electrostatic persistence length, L_E, which varies inversely with the salt concentration. For PSS, L_E is given by[14]

$$L_E \approx 3.5 \times 10^{-2}/\kappa^2 \tag{15}$$

where κ^{-1} is the Debye screening length. L_E is only about 0.3 Å for PSS at a salt concentration of 1 M, rising to 3 Å at 0.1 M, and 30 Å at 0.01 M. For $L_E > L_P$, therefore, adsorbed amounts at equilibrium are expected to increase with increasing salt concentration along with

a decrease in brush height for a given surface coverage, as predicted by eqs 10 and 11. At 1 M salt, charges on the polyelectrolyte are sufficiently screened so that the aggregation properties of the neutral–charged diblocks resemble those of an uncharged diblock in a nonpolar solvent.

Conclusions

This paper describes a preliminary study of the aggregation of poly(*tert*-butylstyrene)–poly(styrenesulfonate) (PtBS–PSS) diblock copolymers at silica surfaces in aqueous solutions of the polymer. The PSS block is charged in solution and hydrophilic, whereas the PtBS block is uncharged and hydrophobic. Two block copolymers with molecular weights 8.7×10^4 and 1.6×10^5 were studied. In both cases, the size of the hydrophobic block is small compared to the size of the hydrophilic block.

In situ ellipsometry measurements using a solution cell indicate that an adsorbed amount cannot be measured in salt-free solutions, demonstrating that electrostatic interactions between charged groups on the polyelectrolyte block inhibit the formation of an adsorbed layer in the absence of charge screening. In 1 M salt solutions, electrostatic interactions are screened sufficiently to allow aggregation at the water surface, and an adsorbed amount can be measured as a function of time. The adsorbed amount at saturation is significantly higher for a diblock with a small hydrophobic group compared with that measured for a polyelectrolyte homopolymer of comparable molecular size, under similar adsorption conditions. This shows that the hydrophobic block plays a significant role in the anchoring of the diblock at the wafer surface. Enhanced adsorption for the diblock copolymers is confirmed with atomic-force microscopy measurements on the adsorbed layers.

The kinetics of adsorption of the diblocks clearly show a two-stage process. At early times, transport of single chains or micellar aggregates to the surface is the only limitation to the growth of the adsorbed layer. The surface layer in this regime is expected to consist of macromolecules that are relatively unperturbed from their configuration as free chains in solution. At later times, interactions between polyelectrolyte blocks tethered to the interface become progressively more important with increasing coverage and the adsorption process slows down. The solvated polyelectrolyte blocks must stretch into the solution to accommodate new chains, creating an activation barrier for further adsorption.

The variation of the adsorbed amount at equilibrium with the size of the polyelectrolyte block can be explained using scaling laws for polyelectrolyte chains anchored to a solid surface by a short hydrophobic block: Larger solvated chains pay a higher elastic penalty for stretching, at a given number density (number of molecules per unit area) at the surface. This favors the adsorption, per unit area and at equilibrium, of around twice as many chains if the polyelectrolyte block size is reduced by half. This is the result that is seen experimentally for the diblock copolymers studied here.

Scaling laws also predict that the equilibrium adsorbed amount for a given system will decrease with decreasing salt concentration, accompanied by an increase in the brush thickness for a given surface coverage. This needs to be studied experimentally, and ellipsometry provides adequate sensitivity for the measurement of adsorbed amounts for these systems. For unique thickness measurements, however, a more sensitive technique than ellipsometry is required. Some work in this regard has already been done using the surface-forces apparatus.[20]

Acknowledgment is made to the donors of the Petroleum Research Fund, administered by the American Chemical Society, for the partial support of this research. Partial support was also received, with appreciation, from the National Science Foundation (Grant NSF/CTS-9107025, Interfacial Transport and Separations Program (CTS) and Polymers Program (DMR). We would like to thank C. Allain, J. F. Argillier, N. Dan, P. Guenoun, F. Pincus, Y. Rabin, L. Yang, and E. Zhulina for helpful discussions. We appreciate the help of M. Stamm and J. Dorgan concerning design of the ellipsometry adsorption cell.

References and Notes

(1) Halperin, A.; Tirrell, M.; Lodge, T. P. *Adv. Polym. Sci.* **1992**, *31*, 100.
(2) Napper, D. *Polymeric Stabilization of Colloidal Dispersions*; Academic Press: London, 1983.
(3) Marques, C.; Joanny, J. F.; Leibler, L. *Macromolecules* **1988**, *21*, 1051.
(4) Johner, A.; Joanny, J. F. *Macromolecules* **1990**, *23*, 5299.
(5) Israëls, R.; Scheutjens, J. M. H.; Fleer, G. J. *Macromolecules* **1993**, *26*, 5405.
(6) Tassin, J. F.; Siemens, R. L.; Yang, W. T.; Hadziioannou, G.; Swalen, J. D.; Smith, B. A. *J. Phys. Chem.* **1989**, *93*, 2106.
(7) Munch, M. R.; Gast, A. P. *Macromolecules* **1990**, *23*, 2313.
(8) Parsonage, E. M.; Tirrell, M.; Watanabe, H.; Nuzzo, R. G. *Macromolecules* **1991**, *24*, 1987.
(9) Motschmann, H.; Stamm, M.; Toprakcioglu, Ch. *Macromolecules* **1991**, *24*, 3681.
(10) Dorgan, J. R. M.; Stamm, M.; Toprakcioglu, Ch.; Jérôme, R.; Fetters, L. J. *Macromolecules* **1993**, *26*, 5321.
(11) de Gennes, P. G.; Pincus, P.; Velasco, R. M.; Brochard, F. *J. Phys. Fr.* **1976**, *37*, 1461.
(12) Odijk, T.; Houwaart, A. C. *J. Polym. Sci., Polym. Phys. Ed.* **1978**, *16*, 627.
(13) Fixman, M.; Skolnick, J. *Macromolecules* **1978**, *11*, 863.
(14) Wang, L.; Yu, H. *Macromolecules* **1988**, *21*, 3498.
(15) Takahashi, A.; Kato, T.; Nasagawa, M. *J. Phys. Chem.* **1967**, *71*, 2001.
(16) Marra, J.; van der Schee, H. A.; Fleer, G. J.; Lyklema, J. In *Adsorption From Solution*; Ottewill, R. H., Rochester, C. H., Smith, A. L., Eds.; Academic Press: New York, 1983.
(17) Dan, N.; Tirrell, M. *Macromolecules* **1993**, *26*, 4310.
(18) Pincus, P. *Macromolecules* **1991**, *24*, 2912.
(19) Borisov, O. V.; Zhulina, E. B.; Birshtein, T. M. *Macromolecules* **1994**, *27*, 4795.
(20) Argillier, J. F.; Mao, G.; Tirrell, M.; Mays, J. *Macromolecules*, submitted.
(21) Ferrieu, F.; Stehle, J. L.; Bernoux, F.; Thomas, O. *Mater. Res. Soc. Symp. Proc.* **1988**, *101*, 403.
(22) Aspnes, D. E.; Studna, A. A. *Appl. Opt.* **1975**, *14*, 220.
(23) Azzam, R. M. A.; Bashara, N. M. *Ellipsometry and Polarized Light*; North-Holland: Amsterdam, 1977.
(24) Hass, G.; Hadley, L. *American Institute of Physics Handbook*, 3rd ed.; McGraw-Hill: New York, 1972.
(25) *CRC Handbook of Chemistry and Physics*, 67th ed.; Weast, R. C., Ed.; CRC Press: Boca Raton, FL, 1987.
(26) Huglin, M. H. In *Polymer Handbook*, 3rd ed.; Brandrup, J., Immergut, E. H., Eds.; Wiley: New York, 1989.
(27) McCrackin, F. L. *NBS Tech. Note* **1969**, *479*.
(28) Frommer, M. A.; Miller, I. R. *J. Chem. Phys.* **1968**, *72*, 1834.
(29) Kawaguchi, M.; Hayashi, K.; Takahashi, A. *Macromolecules* **1984**, *17*, 2066.
(30) Manning, G. S. *J. Chem. Phys.* **1969**, *51*, 924.
(31) Ligoure, C.; Leibler, L. *J. Phys. Fr.* **1990**, *51*, 1313.
(32) Guenoun, P.; Lipsky, L.; Tirrell, M. Manuscript in preparation.
(33) de Gennes, P.-G. *Macromolecules* **1980**, *13*, 1069.
(34) Alexander, S. *J. Phys. (Paris)* **1977**, *38*, 977.

MA946106U